In App. A it was shown that $q \approx 0.5$ leads to particle delocalization and likely makes the system amenable to a mean field description (Fig. 1A.2; see however provisos end paragraph of App. A). In such a case Hartree-Fock approximation is tantamount to a selfconsistent relation between density and potential, weighted by the nucleon-nucleon interaction v (eventual sum of the bare and the induced interaction), i.e.

exp $\sum_i \sigma(0^+_{exc}(i))_{exc} = \sigma_{exc}$

$\frac{\sigma_{exc}}{\sigma_{gs\to gs}} \approx 0.03$ (11)

(31)

1.D. COOPER PAIRS

1.D.1 independent particle motion

~~($q \approx 0.5$), mean field (see Fig. 1.A.2)~~

$$U(r) = \int d\mathbf{r}'\rho(r')v(|\mathbf{r}-\mathbf{r}'|),$$

$$U_x(r,r') = -\sum_i \varphi_i^*(\mathbf{r}')v(|\mathbf{r}-\mathbf{r}'|)\varphi_i(\mathbf{r}'),$$

$$\rho(r) = \sum_i |\varphi(\mathbf{r})|^2; \quad \int d\mathbf{r}\rho(r) = N,$$

leading to ~~Hartree-Fock~~ complete separation between occupied ($|i\rangle$) and empty ($|k\rangle$) states, the Hartree-Fock ground state being

$$\left(U_\nu^2 + V_\nu^2\right) = 1\varphi = \bar{a}_\nu^\dagger|0\rangle = \left(U_\nu + V_\nu a_\nu^\dagger\right)|0\rangle; V_\nu^2 = \begin{cases} 1 & \epsilon_i \le \epsilon_F, \\ 0 & \epsilon_i > \epsilon_F, \end{cases}$$

$$|HF\rangle \; \cancel{|\text{Nilsson}(\Omega)\rangle_{\mathcal{K}}} = \det(\varphi_\nu) = \Pi\bar{a}_\nu^\dagger|0\rangle = \Pi a_i^\dagger|0\rangle = \Pi a_i^\dagger a_{\bar{i}}^\dagger|0\rangle.$$

A - A

$$|\text{IKM}\rangle \sim \int d\Omega \mathcal{D}^I_{MK}(\Omega)|\text{Nilsson}(\Omega)\rangle; \; E_I = (\hbar^2/2\mathcal{I})I(I+1); I = I_{rig}$$

B - B from p. 11d

1.D.2 independent pair motion

from p. 11c Let us make use of the constant matrix element approximation $\langle j_1 j_2|v|j_3 j_4\rangle = G$. The pairing abnormal density of the mean field is related to pair operators (finite value), i.e.,

$$\sum\langle a_{j_2}^\dagger a_{j_1}^\dagger\rangle a_{j_3}a_{j_4} + \sum a_{j_2}^\dagger a_{j_1}^\dagger\langle a_{j_3}a_{j_4}\rangle; \; \varphi^{COOPER} = \left(U_j + V_j a_{jm}^\dagger a_{j\bar{m}}^\dagger\right)|0\rangle,$$

the ground state (mean field) wavefunction being the BCS wavefunction

$$|BCS\rangle = \Pi_{jm>0}\left(U_j + V_j a_{jm}^\dagger a_{j\bar{m}}^\dagger\right)|0\rangle; \; \alpha_0 = \langle BCS|\sum_{jm>0} a_{jm}^\dagger a_{j\bar{m}}^\dagger|BCS\rangle.$$

Introducing the phasing,

$$U_\nu = |U_\nu| = U'_\nu; \; V_\nu = e^{-2i\phi}V'_\nu \; (V'_\nu \equiv |V_\nu|) \; (\nu \equiv j,m); \quad a'^\dagger_\nu = e^{-i\phi}a^\dagger_\nu;$$

here ϕ is the gauge angle, one can write for the intrinsic wavefunction,

$$|BCS(\phi)\rangle_{\mathcal{K}} = \Pi\left(U'_\nu + V'_\nu e^{-2i\phi}a_\nu^\dagger a_{\bar{\nu}}^\dagger\right)|0\rangle = \Pi\left(U'_\nu + V'_\nu a'^\dagger_\nu a'^\dagger_{\bar{\nu}}\right)|0\rangle,$$

$$= |BCS(\phi=0)\rangle_{\mathcal{K}'} : \text{lab. system}, \; \mathcal{K}' : \text{intr. system } \mathcal{K}',$$

The BCS number and gap equations, order parameter and two-nucleon spectroscopic amplitudes are

$$\alpha_0 = \alpha'_0 e^{-2i\phi}; \; \alpha'_0 = \sum_{\nu>0} U'_\nu V'_\nu; \quad B_\nu = \langle BCS|[a'^\dagger_\nu a'^\dagger_\nu]_0|BCS\rangle = (j_\nu + 1/2)^{1/2} U'_\nu V'_\nu.$$

Examples of B_ν coefficients for the reaction $^{124}Sn(p,t)^{122}Sn(gs)$ are given in table 1.D.1

$$\Delta = G\alpha_0; \; N_0 = 2\sum_{\nu>0} V_\nu^2; \; \frac{1}{G} = \sum_\nu \frac{1}{2E_\nu}; \; \left\{\begin{matrix} V'_\nu \\ U'_\nu \end{matrix}\right\} = \frac{1}{\sqrt{2}}\left(1 \mp \frac{1}{E_\nu}\right)^{1/2}$$

$\|$ space

The wave function of the members of a pairing rotational band, can be written as

$$|N_0\rangle \sim \int_0^{2\pi} d\phi|BCS(\phi)\rangle_{\mathcal{K}} \sim \left(\sum_{\nu>0} c_\nu a_\nu^\dagger a_{\bar{\nu}}^\dagger\right)^{N_0/2}|0\rangle; \; E_N = (\hbar^2/2\mathcal{I})N^2 I \approx 2\hbar^2/G$$

In the case of a deformed nucleus, the system acquires not only a priviledged orientation in gauge space, but also in 3D-space. Now, as summarized

a quadrupole

above, in a superfluid system, Cooper pairs and not single particles, are the building blocks of the system. But while the mean (32) square radius of a nucleon at the Fermi energy is $\langle r^2\rangle^{1/2} \approx (3/5)^{1/2} R_0$ ($R_0 = 1.2$ fm ≈ 6 fm ($A \approx 120$)), that of a Cooper pair is determined by the correlation length $\xi \approx \hbar v_F / M_n \approx 36$ fm between the two nucleons forming the pair (within this context see Figs. 1.A.4 and 1.A.5), consequently orienting the quadrupole deformed potential in different directions (angles Ω), will have a ~~much~~ less pronounced effect on Cooper pairs that on independent particles. Within this context one can mention the fact that low-lying (nuclear) collective vibrations (and rotations) are not observed (essentially) at intrinsic excitation energies corresponding to temperatures of $\approx$ 1-2 MeV. In this case, this is because the surface is strongly fluctuating and thus not well define, making it non operative its anisotropic orientation in space.

In keeping with the fact that in FMBS) and due to the important role played by quantal fluctuations deformations are explicated through rotational bands, superfluid nuclei display ~~a~~ well defined pairing rotational bands (e.g. the ground ~~state~~ of the superfluid Sn-isotopes). The moment of inertia is directly

see Fig. 1.3

related to the effective pairing interaction, (41)
eventually sum of the bare and of the induced interactions. These rotational bands are specifically excited in two-nucleon transfer reactions (cf. Figs. 1.3, 1.4)

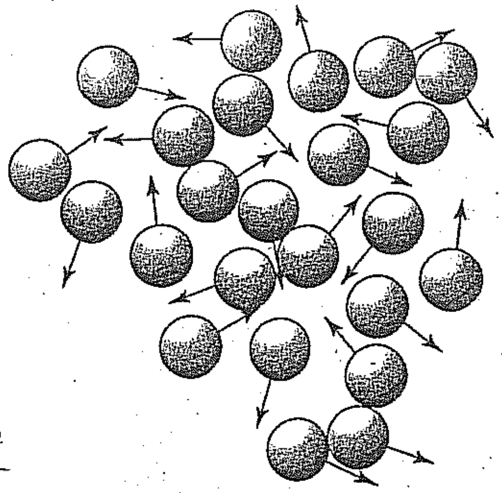

1.A.4

Figure ~~1.13~~. A system of independent Cooper pairs (Schafroth pairs). This situation corresponds to the incoherent solution of the many Cooper pair problem, the so called Fock state.
In cold gases the system after the Feshbach resonance leading to BEC

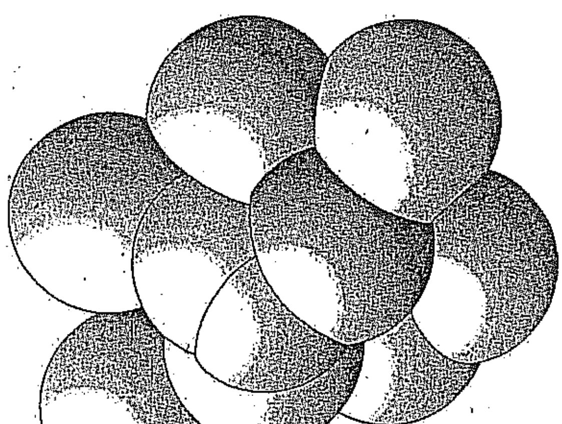

1.A.5

Figure ~~1.14~~. There are about 10^{18} Cooper pairs per cm^3 in a superconducting metal. A Cooper pair has a spatial extension of about 10^{-4} cm. Thus a given Cooper pair will overlap with 10^6 other Cooper pairs, leading to strong pair–pair correlation, as schematically shown. This solution corresponds to the coherent solution of the many Cooper pair problem (coherent state), also valid in atomic nuclei.

fluids (pairing vibrations, the right physics) (11) C

(E) From this vantage point one can posit that it is not so much ~~the~~ or at least not only the nuclear superfluid state which is abnormal, but the normal (closed shell) system ~~s~~ (see App. D).

p. 4 version June 6/14 (E) (34)

(A) - (A) p. 11

Fig. 5 WSPC Spont. Symm breaking II

~~The above self consistent~~

(where Q_{2M} ... is the quadrupole operator)

In the case in which $\langle Q_{2M}\rangle = 0$ the system can display ~~quadrupole~~ a spectrum of quadrupole vibrations; the associated ZPF leads to dynamic violation ~~of quadru~~ of rotational invariance

(A) To be solved, the above selfconsistent ~~equation~~ equation have to be given boundary conditions. ~~Namely~~ In particular whether the system has a spherical or a, ~~e.g.~~ for example, quadrupole deformed shape. That is, whether $\langle HF|Q_2|HF\rangle$ ~~is~~ is zero or ~~different~~ or has a finite value ~~...~~ ~~the operat~~, ~~where~~

(cf. App H relation between collectivity and correls. rots ⟷ vibs)

$$Q_{2M} = \sum_{j_1 j_2} \langle j_2 | r^2 Y_{2M} | j_1 \rangle \left[a^\dagger_{j_1} a_{j_2}\right]_{2M}$$

($\beta = 0$, ...)

being the quadrupole operator. In the case in which ~~...~~ $\langle Q_{2M}\rangle \neq 0$, the $|HF\rangle$ state is known ~~as~~ as the Nilsson state, ~~...~~ $|Nilsson(\Omega)\rangle_K$ defining a priviledged orientation in 3D space and thus an intrinsic, body-fixed system of reference K' which makes ~~an~~ an angle Ω (Euler angles) with the laboratory frame K. ~~The fluctuation associated~~ ~~...~~ ~~The fluctuations associated of the ang~~ Because there is no restoring force associated with the different orientations, (~~different...~~ fluctuation in Ω diverge ~~leading a to a restoration of symmetry~~ ($C \to 0$, D finite in the case of low-lying collective, large amplitude vibrations mentioned above) leading to a rotational band ~~a~~ displaying a rigid moment of inertia and whose members are the states (A) p. (11) (version 6/7/14)

carrying ~~ϕ~~ particle (range) ... entire number ($\beta = 0$) ~~ϕ~~ keeping with its ~~particle~~ particle-hole character

correlation and fluctuation ...

type by E. Vig.

p. 1c / Cf. Fig. 1.A.

(B) Similar dynamic and ~~static~~ spontaneous symmetry breaking phenomena takes place in connection with particle-particle $(\beta=+2)$ ~~and~~ hole-hole $(\beta=-2)$ correlations, that is ~~with~~ gauge space, (see ~~Table~~ Fig. 1.D.1), ~~These~~ subjects discussed in App. E (~~pairing~~ dynamic: pairing vibrations) and below (static: pairing rotations) (see also Figs. 1.1 and 1.3) ~~to~~ (11)d

(B) p. 11 version 6/7/14

(35)

36

11 e

~~the successive contribution to the two-particle transfer cross section is the dominant one, non-orthogonality canceling much of the already weak, simultaneous contribution. Of notice that similar issues were debated in connection with the proposal of Josephson[29] concerning the possibility of observing a supercurrent across a dioxide layer separating two superconductors, and Bardeen's objection that the pairing gap is zero inside the layer.[30] The answer to such an objection is to be found in the fact that it is α_0 $(= \langle P^\dagger \rangle)$ which controls tunneling and not Δ, a fact that emerges naturally from Gorkov's formulation of superconductivity (see contribution of Potel and Broglia to the present volume).~~

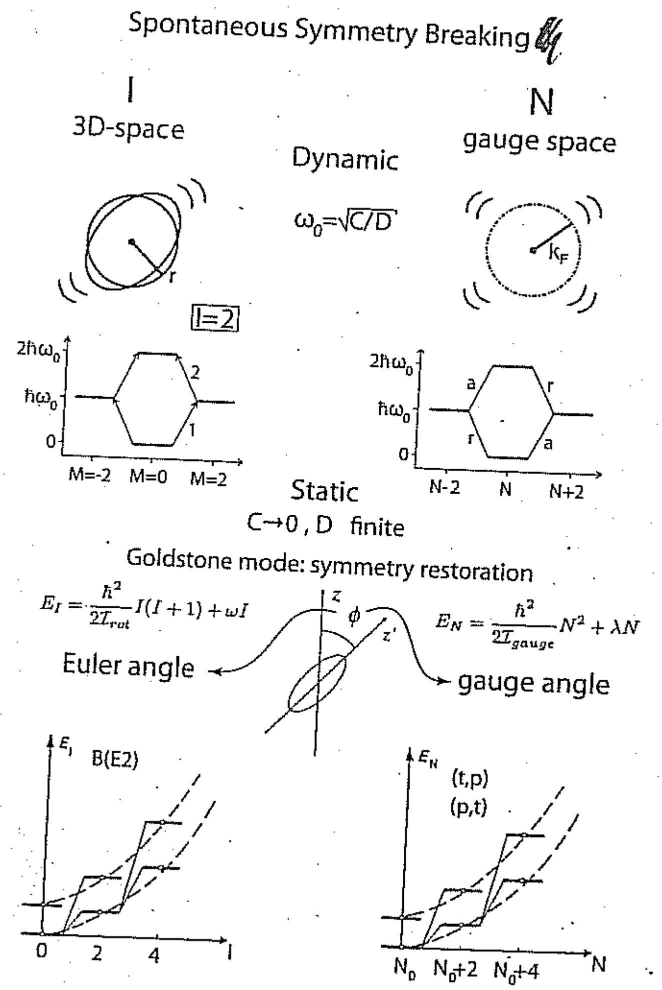

1.D.1

rotational band, FMBS fingerprint of deformation

Fig. 1. Schematic representation of collective modes associated with dynamical and static distortions violating rotational and gauge symmetries (see also table XI in Ref. 4)

Broglia et al (1973)

1.D.3 Two-nucleon spectroscopic amplitudes associated with transitions between members of a pairing rotational band

Explain in this appendix
pairing rots + p. vibs.
(refer Advance, two-entry

Table 1.A.1
Chapter Transfer
nutshell
wave function
Covello

use all three w.fs
p. 31

Pair transfer in
a nutshell Chapt. 1

large ampl. pair. vib.

Two-entry
Table WSPC Table 5
p. 1652

+ Figs

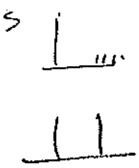

talk
Padova

37

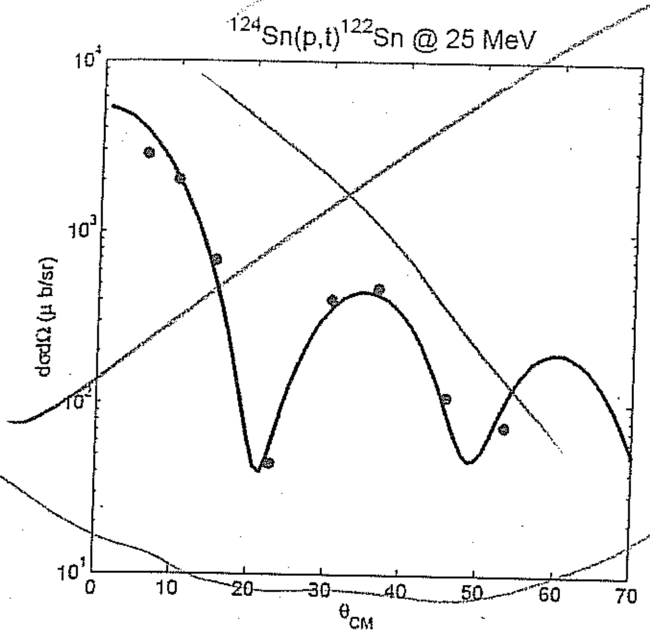

38

see also next page

Table. 1.D.1

Figure 1.A.3:

Covello

spectroscopic amplitude $\sqrt{j_\nu + 1/2}\; U_\nu(A) V_\nu(A+2)$

↑ check

is it $\sqrt{2}\,\Omega_\nu$ or $\sqrt{\Omega_\nu}$?

$\sqrt{2}\,\Omega$

	2n spectr. ampls. ^{124}Sn(p,t)^{122}Sn(gs)		
$nlj^{a)}$	BCS$^{b)}$	NuShell$^{c)}$	$V^{d)}_{low-k}$
$1g_{7/2}$	0.44	0.63	− 1.1673
$2d_{5/2}$	0.35	0.60	−0.7556
$2d_{3/2}$	0.58	0.72	−0.4825
$3s_{1/2}$	0.36	0.52	− 0.3663
$1h_{11/2}$	1.22	-1.24	− 0.6647

Table 1.A.1: **a)** quantum numbers of the two-particle configurations $(nlj)^2_{J=0}$ coupled to angular momentum $J = 0$. **b)** $\langle BCS|P_\nu|BCS\rangle = \sqrt{2j_\nu + 1}U_\nu(A)V_\nu(A + 2)$ $(A + 2 = 124)$ where $P_\nu = a_{\tilde\nu}a_\nu(\nu \equiv nlj)$ (cf. Potel et al. (2011, 2013a,b)). **c)** Two-neutron overlap functions obtained making use of the shell-model wavefunctions for the ground state of ^{122}Sn and ^{124}Sn and the code NuShell (Brown and Rae, 2007) (cf. also ?). The wavefunctions were obtained starting with a G matrix derived from the *CD*-Bonn nucleon-nucleon interaction Machleidt et al. (1996). These amplitudes were used in the calculation of ^{124}Sn(p,t)^{122}Sn absolute cross sections carried out by I.J. Thompson (Thompson, 2013).

Snej Table IV Covello

PR C 74 (2006) 054605

Objection

What about $v_{pairing}(= G)$ becoming zero, e.g. between the two nuclei?

part of Table 1.P.1

39

Table 1. Two-neutron overlap function for $\langle ^{122}\mathrm{Sn}|^{124}\mathrm{Sn}\rangle$.

$1g_{7/2}^2$	0.62944
$2d_{5/2}^2$	0.59927
$2d_{3/2}^2$	0.71913
$3s_{1/2}^2$	0.51892
$1h_{11/2}^2$	−1.24399

of ($0g_{7/2}$, $1d_{5/2}$, $1d_{3/2}$, $2s_{1/2}$, $0h_{11/2}$) for neutrons with the code NuShell.[24] The model-space two-body matrix elements are those used in Refs. 29 and 30. They were obtained starting with a G matrix derived from the CD-Bonn[31] nucleon–nucleon interaction. The harmonic oscillator basis was employed for the radial wave functions with an oscillator energy $\hbar\omega = 7.87$ MeV. The effective interaction for the above shell-model space is obtained from the Q-box method and includes all non-folded diagrams through third-order in the interaction G to sum up the folded diagrams to infinite order.[32,33] The single-particle energies were adjusted to reproduce the observed states in ^{131}Sn.

The inputs to the reaction code are the two-nucleon spectroscopic amplitudes (TNA) of Table 1. A center of mass correction[34] equal to $[A/(A-2)]^{2n+\ell}$ for the TNA has been applied, where $A = 124$. Our sign convention is that the radial wave functions are positive at the origin. The sequential process was calculated by a single intermediate state for each of these orbits connected by a product of one-nucleon spectroscopic amplitudes that are equal to the center-of-mass corrected TNA multiplied by $\sqrt{2}$ that takes into account the normalization of the two-particle amplitude. Future calculations should also take into account the TNA obtained from the mixing of neutron pairs for orbitals outside of the model space.

We use the triton potential of Li,[35] the deuteron potential of Daehnick,[36] and the proton potential of Chapel Hill 89.[37] All the two-neutron wave functions are constructed within the half-separation-energy prescription. For a triton wave function we use the pure s^2 configuration found by the product of eigenstates at the half-separation energy (4.24 MeV) in a Woods–Saxon potential with $V = 77.83$ MeV, $R = 0.95$ fm, and $a = 0.65$ fm (the results are not sensitive to these values). The Sn wave functions shown in Table 1 are found at the half-separation energy (7.219 MeV) in a WS potential with $r = 1.17$ fm, and $a = 0.75$ fm that has the fixed spin-orbit component $V_{so} = 6.2$ MeV, $r = 1.01$ fm, and $a = 0.75$ fm.

The complete cross section prediction is shown in Fig. 1, compared with the experimental data of Guazzoni *et al.*[28] Now we see that, with the shell-model overlaps and proper finite-range and sequential contributions, the unhappiness factors are much closer to unity. A better agreement between theory and experiment has already been published,[19] but in the present calculations there are still questions about the angular oscillations which are in not so good agreement with experiment. Note that Guazzoni *et al.*[28] took the better agreement of the *simultaneous* transfer

(See Figs gregory)

40

Covello + Thompson 02/09/2013 11:34

02/09/2013 9:28

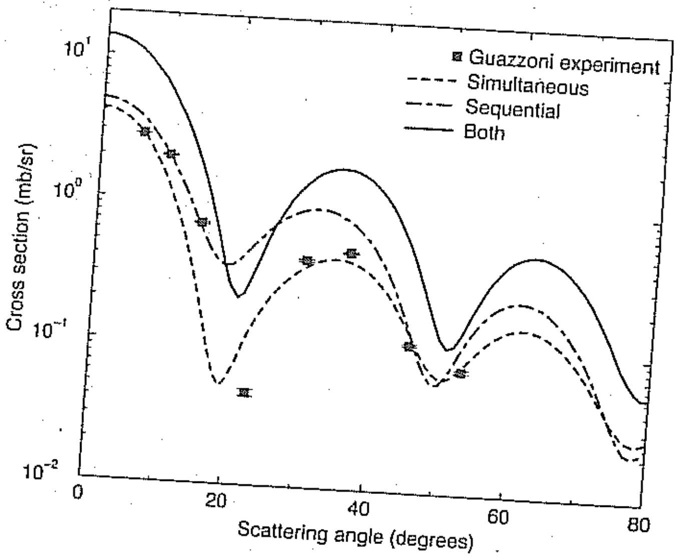

Fig. 1. Simultaneous (short dash), sequential (dot-dash) and simultaneous + sequential (solid line) cross sections for the reaction ^{124}Sn(p,t)^{122}Sn at 25 MeV, in comparison with the experimental data of Guazzoni *et al.*[28]

curve (dashed line) to indicate small effects for sequential transfers, but this is not correct since we do know that sequential transfers occur, and can calculate them with good accuracy in this model (dot-dashed line).

To see the importance of the nonorthogonality terms, and hence of choosing 'prior–post' couplings if nonorthogonality terms are to be avoided, Fig. 2 plots the different sequential cross sections for all possible combinations of post and prior for the two steps. The prior–post solid curve is the dot-dashed curve in Fig. 1. The other curves are all different from this one, and cannot be simply added to the simultaneous amplitude to get the correct result. This also implies that no complete calculation with only zero-range couplings is possible.

Finally, it is instructive to look at the interference effects between the various simultaneous and sequential contributions. To display these coherence effects, I choose to plot the scattering amplitude at zero degrees for the non-spin-flip amplitude $m_p = m_t = 1/2$ (the only nonzero amplitude at this angle). Figure 3 plots all the simultaneous and sequential contributions from the different components listed in Table 1, along with their coherent sums. We see that all the contributions to the simultaneous transfer are constructively coherent, as are all the contributions to the total sequential amplitude. This constructive coherence follows from the signs of the amplitudes in Table 1, and reflects the significant pairing enhancement in ^{124}Sn. The total sequential and simultaneous amplitudes are not uniformly coherent with each other, however. A uniform 90° angle between the simultaneous and sequential amplitudes in Fig. 3 would indicate an incoherent summation of the two

Appendix 1.E Two–nucleon spectroscopic amplitudes associated with pairing vibrational modes in closed shell systems: the ^{208}Pb case.

The solution of the pairing Hamiltonian

$$H = H_{sp} + H_p,$$

where

$$H_{sp} = \sum_{\nu} \epsilon_\nu a_\nu^\dagger a_\nu$$

and

$$H_p = -GP^\dagger P,$$

with

$$P^\dagger = \sum_{\nu>0} a_\nu^\dagger a_{\bar{\nu}}^\dagger,$$

for the case of closed shell systems and in the harmonic approximation (RPA) leads to pair addition (a) pair removal (r) two–particle, two–hole correlated modes, the associated creation and annihilation operator being

$$\Gamma_a^\dagger(n) = \sum_k X_n^a(k)\Gamma_k^\dagger + \sum_i Y_n^a(i)\Gamma_i$$

and

$$\Gamma_r^\dagger(n) = \sum_i X_n^r(i)\Gamma_i^\dagger + \sum_k Y_n^r(k)\Gamma_k,$$

with

$$\sum X^2 - Y^2 = 1$$

and

$$\Gamma_k^\dagger = a_k^\dagger a_{\bar{k}}^\dagger, \quad (\epsilon_k > \epsilon_F),$$

and

$$\Gamma_i^\dagger = a_{\bar{i}} a_i, \quad (\epsilon_i \leq \epsilon_F).$$

The relations

$$[H, \Gamma_a^\dagger(n)] = \hbar W_n(\beta = +2)$$

and

$$[H, \Gamma_r^\dagger(n)] = \hbar W_n(\beta = -2),$$

where β is the transfer quantum number, while n labels the roots of the corresponding dispersion relations in increasing order of energy,

$$\frac{1}{G(\pm 2)} = \sum_k \frac{(\Omega_k/2)}{2\epsilon_k \mp W_n(\pm 2)} + \sum_i \frac{(\Omega_i/2)}{2\epsilon_i \pm W_n(\pm 2)},$$

Pair vibration

1.E. TWO–NUCLEON SPECTROSCOPIC AMPLITUDES ~~ASSOCIATED WITH PAIRING VIBRATIONAL~~

i ϵ_i

i $|\epsilon_i|$

42

orbit	ϵ_j	$\epsilon_{p_{1/2}} - \epsilon_k \equiv \|\epsilon_k\| - \|\epsilon_{p_{1/2}}\|$
$0h_{9/2}$	-10.62	3.47
$1f_{7/2}$	-9.50	2.35
$0i_{13/2}$	-8.79	1.64
$2p_{3/2}$	-8.05	0.90
$1f_{5/2}$	-7.72	0.57
$2p_{1/2}$	-7.15	0
$\epsilon_F = -5.825$ keV		$\epsilon_k - \epsilon_{g_{9/2}} \equiv \|\epsilon_{g_{9/2}}\| - \|\epsilon_k\|$
$1g_{9/2}$	-3.74	0.
$0i_{11/2}$	-2.97	0.77
$0j_{15/2}$	-2.33	1.41
$2d_{5/2}$	-2.18	1.56
$3s_{1/2}$	-1.71	2.03
$1g_{7/2}$	-1.27	2.47
$2d_{3/2}$	-1.23	2.51

Table 1.E.1: Valence single particle levels of ^{208}Pb. In the upper part the occupied levels ($\epsilon_i \leq \epsilon_F$) are shown while in the lower part the empty levels ($\epsilon_k > \epsilon_F$). Of notice that $\epsilon_{p_{1/2}} - \epsilon_{g_{9/2}} = 3.41$ MeV, is the single–particle gap associated ~~associated~~ with the $N = 126$ shell closure.

of the system under study (^{208}Pb in the present case).

. It is of notice that

where $\Omega_j = j + 1/2$ is the pair degeneracy.

For the case of the (neutron) pair addition and pair substraction modes of ^{208}Pb the above equation ~~can be~~ are solved graphically (cf. Fig 1.E.1) in minimum of the dispersion relation ~~defining~~ defines the Fermi energy. This is in keeping with the fact that in the case in which $W_1(\beta = +2) = W_1(\beta = -2) = 0$, corresponding to the phase transition between normal and superfluid phases, ~~in which case~~ the Fermi energy value is well defined, ~~the~~ BCS λ variational parameter ~~coincides with ϵ_F~~. It is of notice that, as a rule the Fermi energy of closed shell nuclei is defined as half the energy difference between the last occupied and the first empty single particle state (cf. e.g. Mahaux ?). ~~One then obtains~~ Making use of the values (see Fig 1.E.1)

The energy value at which the dispersion relation touches for the first time the corresponding axis, coincide with the

$$\begin{cases} E_{corr}(+2) = B(208) + B(210) - 2B(209) = 1.248\,\text{MeV}\,, \\ E_{corr}(-2) = B(208) + B(206) - 2B(207) = 0.630\,\text{MeV}\,, \end{cases}$$

One obtains

$W_1(+2) + W_1(-2) = (B(208) - B(206)) - (B(210) - B(208)) = 14.11 - 9.115 = 4.995$ MeV. It is of notice that in the above derivations all ~~the~~ energy difference are > 0. In particular, (see Table 1.E.1)

$$\epsilon_i < \epsilon_F \Rightarrow \epsilon_F - \epsilon_i = -|\epsilon_F| + |\epsilon_i| = |\epsilon_i| - |\epsilon_F| > 0\,,$$

and

$$\epsilon_k > \epsilon_F \Rightarrow \epsilon_k - \epsilon_F = -|\epsilon_k| + |\epsilon_F| = |\epsilon_F| - |\epsilon_k| > 0\,,$$

43

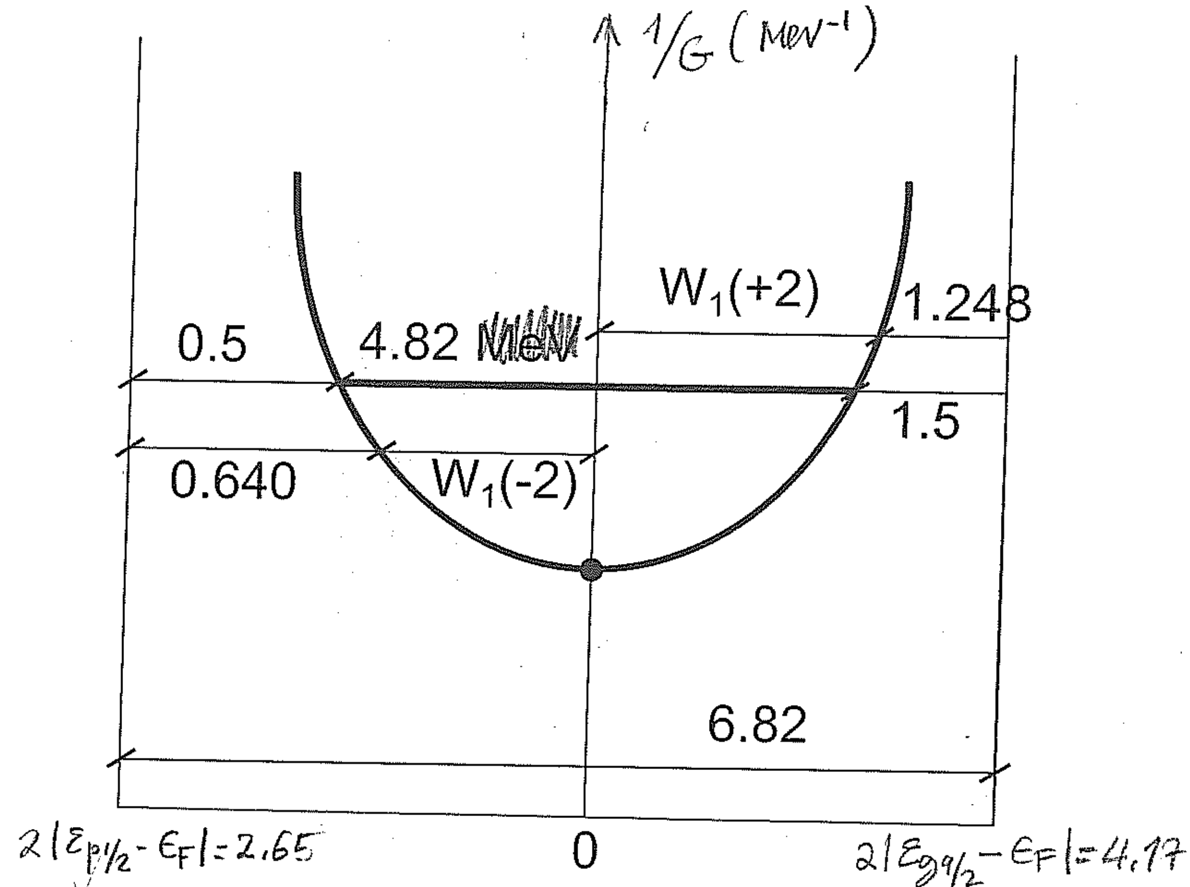

Figure 1.E.1: The right hand side of the RPA pairing vibrational dispersion relation for neutrons in the case of the closed shell system ^{208}Pb ~~(cf. ?)~~ in the region between the two neighboring shells ($p_{1/2}$ and $g_{9/2}$). All quantities are in MeV. For each G there is a straight horizontal line, which is divided by the ~~the~~ curve in three sections. The first one from the left corresponds to the pairing correlation energy of the nucleus ^{206}Pb (two correlated neutron hole states) while the last segment to the right measures the pairing correlation energy of ^{210}Pb (two correlated neutrons above closed shell), the intermediate segment measures the energy of the two phonon pairing vibrational state $(2p-2h)$ of ^{208}Pb. (Bes and Broglia, 1966)

Thus,

$$\left\{ \begin{array}{l} 2(\epsilon_F - \epsilon_{p_{1/2}}) = W_1(-2) + E_{corr}(-2) > 0 \\ 2(\epsilon_{g_{9/2}} - \epsilon_F) = W_1(+2) + E_{corr}(+2) > 0 \end{array} \right\}$$

From Fig. 1.E.1 one can write,

$$2(\epsilon_{g_{9/2}} - \epsilon_F) = W_1(+2) + E_{corr}(+2),$$

¶

and ~~thus~~

$$4.17\text{MeV} = 2(-3.74\text{MeV} - (-5.825)\text{MeV}) = W_1(+2) + 1.248\text{MeV}.$$

Consequently,

$$W_1(-2) = 2.01\text{MeV}, \quad W_1(+2) + W_1(-2) = 4.93\text{MeV}.$$

Let us make a rigid shift of energies setting $\epsilon_F = 0$. Thus,

$$W_1(+2) = 2\epsilon_{g_{9/2}} - E_{corr}(+2) \quad W_1(-2) = -2\epsilon_{p_{1/2}} - E_{corr}(-2).$$

1.E.1 Pair removal mode

In Fig. 1.E.2 the graphical representation of the forwards going RPA amplitude of the pair removal mode is shown. Its expression is

$$X_1^r(i) = \frac{\frac{1}{2}\Omega_i^{1/2}\Lambda(-2)}{2(\epsilon_F - \epsilon_i) - W_1(-2)},$$

where

$$\begin{aligned} 2(\epsilon_F - \epsilon_i) - W_1(-2) &= 2(\epsilon_F - \epsilon_i) - 2(\epsilon_F - \epsilon_{p_{1/2}}) - E_{corr}(-2) \\ &= 2(\epsilon_{p_{1/2}} - \epsilon_i) + E_{corr}(-2) = 2(|\epsilon_i| - |\epsilon_{p_{1/2}}|) + E_{corr}(-2). \end{aligned}$$

Thus,

$$X_1^r(i) = \frac{\frac{1}{2}\Omega_i^{1/2}\Lambda(-2)}{2(|\epsilon_i| - |\epsilon_{p_{1/2}}|) + E_{corr}(-2)}.$$

Making use of the empirical value of $E_{corr}(-2)$ worked out above one obtains,

$$X_1^r(i) = \frac{\frac{1}{2}\Omega_i^{1/2}\Lambda(-2)}{2(|\epsilon_i| - |\epsilon_{p_{1/2}}|) + 0.640\text{MeV}}.$$

0.640

In Fig. 1.E.3 we display the graphical process associated with the backwards going RPA amplitude,

$$Y_1^r(k) = \frac{\frac{1}{2}\Omega_k^{1/2}\Lambda(-2)}{2(\epsilon_k - \epsilon_F) + W_1(-2)}.$$

Making use of

(45)

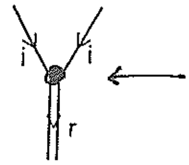

Figure 1.E.2: NFT representation of the forwards going RPA amplitude of the pair removal mode (double downward going arrowed line) describing a two correlated hole state (single downward going arrowed line for each hole with quantum numbers collectively labeled i).

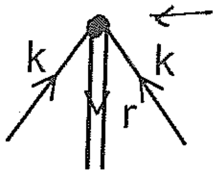

Figure 1.E.3: Same as Fig. 1.E.2 but for the backwards going amplitudes.

$$2(\epsilon_k-\epsilon_F)+2(\epsilon_F-\epsilon_{p_{1/2}})-E_{corr}(-2)=2(\epsilon_k-\epsilon_{p_{1/2}})-E_{corr}(-2)$$
$$=2(|\epsilon_{p_{1/2}}|-|\epsilon_k|)-E_{corr}(-2)=2(|\epsilon_{p_{1/2}}|-|\epsilon_{g_{9/2}}|)+2(|\epsilon_{g_{9/2}}|-|\epsilon_k|)-E_{corr}(-2);$$

~~O~~o ne can write,

$$Y_1^r(k)=\frac{\frac{1}{2}\Omega_k^{1/2}\Lambda(-2)}{2(|\epsilon_{g_{9/2}}|-|\epsilon_k|)+2(|\epsilon_{p_{1/2}}|-|\epsilon_{g_{9/2}}|)-E_{corr}(-2)}$$

with the help of the relation

to finally obtain, ~~making use of~~ $2(|\epsilon_{p_{1/2}}|-|\epsilon_{g_{9/2}}|)-E_{corr}(-2)=6.82\text{MeV}-0.640\text{MeV}=6.18\text{MeV}$, the expression

$$Y_1^r(k)=\frac{\frac{1}{2}\Omega_k^{1/2}\Lambda(-2)}{2(|\epsilon_{g_{9/2}}|-|\epsilon_k|)+6.18\,\text{MeV}}.$$

Because (see Fig. 1.A.1)

The above calculated expressions of $X_1^r(i)$ and $Y_1^r(k)$ contain the experimental values of the 2–hole correlation energies (0.640 MeV). ~~in keeping with the fact that~~ the associated values of G does not lead to the observed correlation energy of the pair addition mode (1.248 MeV), we prefer to choose a single intermediate value and use the resulting $E_{corr}(-2)$ (=0.5 MeV) and $E_{corr}(+2)$ (=1.5 MeV), and calculate with these values the corresponding X, Y amplitudes for both the lowest removal and lowest addition pairing modes. Thus, ~~making use of~~ from

$$X_1^r(i)=\frac{\frac{1}{2}\Omega_i^{1/2}\Lambda(-2)}{2(|\epsilon_i|-|\epsilon_{p_{1/2}}|)+E_{corr}(-2)};\quad Y_1^r(k)=\frac{\frac{1}{2}\Omega_k^{1/2}\Lambda(-2)}{2(|\epsilon_{g_{9/2}}|-|\epsilon_k|)+2(|\epsilon_{p_{1/2}}|-|\epsilon_{g_{9/2}}|)-E_{corr}(-2)}$$

~~and of~~ and

$$2(|\epsilon_{p_{1/2}}|-|\epsilon_{g_{9/2}}|)=6.82\,\text{MeV};\quad 2(|\epsilon_{p_{1/2}}|-|\epsilon_{g_{9/2}}|)-E_{corr}=(6.82-0.5)\,\text{MeV}=6.32\,\text{MeV},$$

(Tamm - Dancoff ; TD)

It is of notice that the coupling strength $\Lambda(-2)$ with which the pair removal mode couples to the single-particle (hole) states is calculated by normalizing the amplitudes: 1) $\sum_i A^2(i) = 1.5549$ MeV^{-2} and thus $\Lambda(-2) = 0.802$ MeV, $\sum (X_1^r(i))^2_{TD} = 1$; 2) RPA, $\Lambda_1^2(-2)(\sum_i A^2(i) - \sum_k B^2(k)) = \Lambda_1^2(-2) \times 1.45073$

1.E. TWO–NUCLEON SPECTROSCOPIC AMPLITUDES ASSOCIATED WITH PAIRING VIBRATIONAL

(46)

units		MeV	MeV^{-1}	RPA	TD
nlj	Ω_i	$\lvert\epsilon_i\rvert - \lvert\epsilon_{p_{1/2}}\rvert$	$A(i)^{a)} = \frac{\frac{1}{2}\Omega_i^{1/2}\Lambda(-2)}{2(\lvert\epsilon_i\rvert - \lvert\epsilon_{p_{1/2}}\rvert)+0.5\text{ MeV}}$	$X_1^r(i)^{b)}$	$X_1^r(i)^{c)}$
$2p_{1/2}$	1	0	1	0.83	0.80
$1f_{5/2}$	3	0.57	0.528	0.44	0.42
$2p_{3/2}$	2	0.90	0.307	0.25	0.25
$0i_{13/2}$	7	1.64	0.350	0.29	0.28
$1f_{7/2}$	4	2.35	0.192	0.16	0.15
$0h_{9/2}$	5	3.47	0.150	0.12	0.12

Table 1.E.2: Forwards going RPA amplitudes of the pair removal mode of ^{208}Pb (i.e., the $|^{206}$Pb(gs)⟩ state), cf. Table XVI Broglia et al. (1973).

Thus $\Lambda(-2) = 0.830$

The above results show that there is a few percentage difference between the two values of Λ (TD and RPA) as well as for the corresponding X-amplitudes. Nonetheless, ground state correlations as expressed by the Y-amplitudes, integrated give rise to a 50% increase in the ^{206}Pb(t,p)^{208}Pb(gs) absolute cross section, from 0.34 mb to 0.52 mb, to be compared with the experimental data ($\sigma = 0.68 \pm 24$ mb), see Fig. 1.E.4

$$\frac{0.830 - 0.802}{0.028} \qquad \frac{0.028}{0.8} \approx 4\%$$

units		MeV	MeV^{-1}	
nlj	Ω_k	$\lvert\epsilon_{g_{9/2}}\rvert - \lvert\epsilon_k\rvert$	$B(k) = \frac{\frac{1}{2}\Omega_i^{1/2}\Lambda(-2)}{2(\lvert\epsilon_{g_{9/2}}\rvert - \lvert\epsilon_k\rvert)+6.23\text{ MeV}}$	$Y_1^r(i)$
$1g_{9/2}$	5	0	0.179	-0.15
$0i_{11/2}$	6	0.77	0.158	-0.13
$0j_{15/2}$	8	1.41	0.156	-0.13
$2d_{5/2}$	3	1.56	0.093	-0.08
$3s_{1/2}$	1	2.03	0.046	-0.04
$1g_{7/2}$	4	2.47	0.090	-0.07
$2d_{3/2}$	2	2.51	0.063	-0.05

Table 1.E.3: Same as Table 1.E.2 but for the ~~backwards~~ amplitude.

Fig. sem. gregory

One can write,

$|^{206}$Pb(gs)⟩

$$\begin{cases} X_1^r(i) = \frac{\frac{1}{2}\Omega_i^{1/2}\Lambda(-2)}{2(|\epsilon_i|-|\epsilon_{p_{1/2}}|)+0.5\text{ MeV}}, \\ Y_1^r(k) = \frac{\frac{1}{2}\Omega_k^{1/2}\Lambda(-2)}{2(|\epsilon_{g_{9/2}}|-|\epsilon_k|)+6.23\text{ MeV}}. \end{cases}$$

Tables 1.E.2 and 1.E.3 ~~thus~~ contain the amplitudes of the pair removal mode of ^{208}Pb ($\Gamma_r^\dagger(1) = \sum X_1^r(i)\Gamma_i^\dagger + \sum Y_1^r(k)\Gamma_k$), that is the two neutron hole correlated state describing $|^{206}$Pb⟩ $= \Gamma_r^\dagger(1)|0\rangle$.

(B) Let us conclude this appendix by noting that ~~It is of notice that~~ while the harmonic (RPA) description of the pair vibrational mode of ^{208}Pb provides a fair description of the two neutron transfer spectroscopic amplitudes, in keeping with the collective character of these (coherent) states, conspicuous anharmonicities in the multi phonon spectrum have been observed and calculated (cf. for example Flynn, Bortignon, Clark).

to p. 19

(B) to p. 19

47

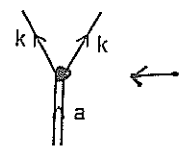

Figure 1.E.~~4~~5: Same as Fig. 1.E.2 but for the pair addition mode

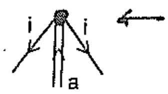

Figure 1.E.~~5~~6: Same as Fig. 1.E.3 but for the pair addition mode

1.E.2 Pair addition modes

In Figs. 1.E.~~4~~5 and 1.E.~~5~~6 the X and Y amplitudes of the pair addition mode are given. The associated expressions are, ~~given below~~:

$$X_1^a(k) = \frac{\frac{1}{2}\Omega_k^{1/2}\Lambda_1(+2)}{2(\epsilon_k - \epsilon_F) - W_1(+2)},$$

which, making use of

$$\begin{aligned}2(\epsilon_k - \epsilon_F) - W_1(+2) &= 2(\epsilon_k - \epsilon_F) - 2(\epsilon_{g_{9/2}} - \epsilon_F) - E_{corr}(+2)\\ &= 2(\epsilon_k - \epsilon_{g_{9/2}}) + E_{corr}(+2) = 2(|\epsilon_{g_{9/2}}| - |\epsilon_k|) + E_{corr}(+2)\end{aligned}$$

can be written as

$$X_1^a(k) = \frac{\frac{1}{2}\Omega_k^{1/2}\Lambda_1(+2)}{2(|\epsilon_{g_{9/2}}| - |\epsilon_k|) + W_1(+2)}.$$

Similarly,

$$Y_1^a(i) = \frac{\frac{1}{2}\Omega_i^{1/2}\Lambda_1(+2)}{2(\epsilon_F - \epsilon_i) + W_1(+2)}.$$

which with the help of the relation, ~~Making use of the relation~~

$$\begin{aligned}2(\epsilon_F - \epsilon_i) + W_1(+2) &= 2(\epsilon_F - \epsilon_i) - 2(\epsilon_{g_{9/2}} - \epsilon_F) - E_{corr}(+2)\\ &= 2(\epsilon_{p_{1/2}} - \epsilon_i) + 2(\epsilon_{g_{9/2}} - \epsilon_{p_{1/2}}) - E_{corr}(+2)\\ &= 2(|\epsilon_i| - |\epsilon_{p_{1/2}}|) + 2(|\epsilon_{p_{1/2}}| - |\epsilon_{g_{9/2}}|) + E_{corr}(+2),\end{aligned}$$

can be written as

$$Y_1^a(i) = \frac{\frac{1}{2}\Omega_i^{1/2}\Lambda_1(+2)}{2(|\epsilon_i| - |\epsilon_{p_{1/2}}|) + 2\Delta\epsilon_{sp} - E_{corr}(+2)}.$$

Making use of $E_{corr}(+2) = 1.5$ MeV (cf. Fig. 1.E.1) and

$$\Delta\epsilon_{sp} = 2(|\epsilon_{p_{1/2}}| - |\epsilon_{g_{9/2}}|) = 6.28\,\text{MeV},$$

48

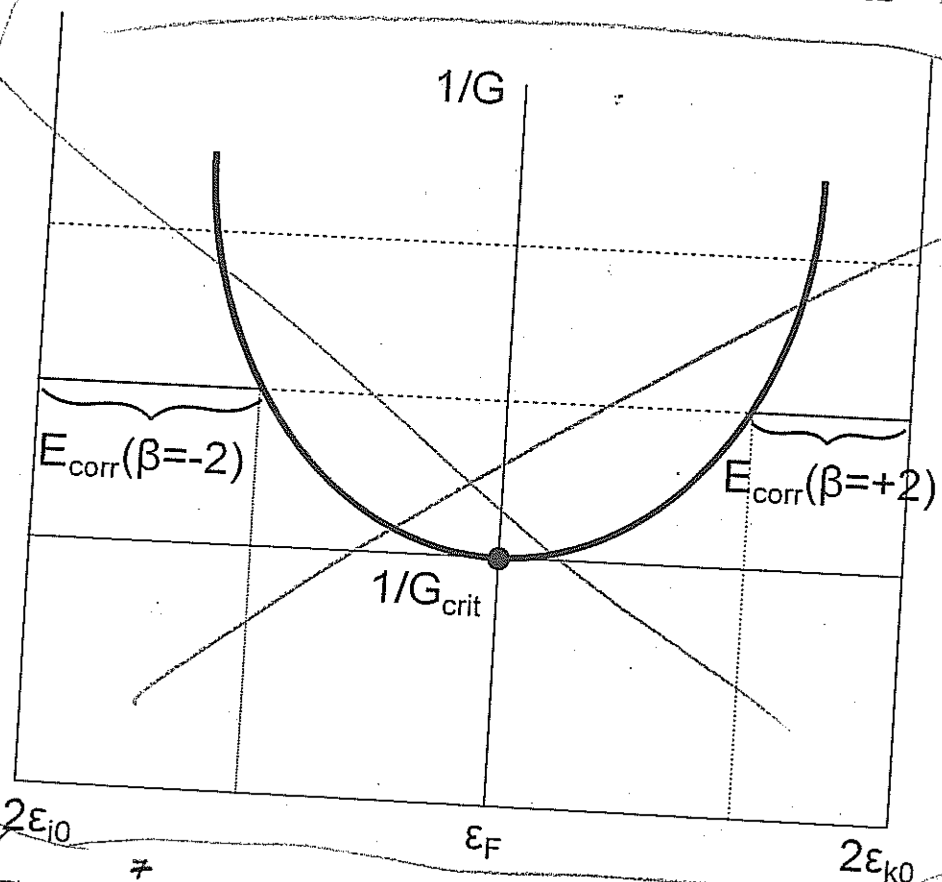

Figure 1.E.~~6~~ 7: Same as Fig. 1.E.1 but schematically emphasizing the different elements characterizing the pairing vibration dispersion relation.

one

~~One~~ thus obtains $2\Delta\epsilon_{sp} - E_{corr}$ (+2) $= (6.82 - 1.5)$ MeV=5.32 MeV, leading to

$$\begin{cases} X_1^a(k) = \dfrac{\frac{1}{2}\Omega_k^{1/2}\Lambda(-2)}{2(|\epsilon_{g_{9/2}}|-|\epsilon_k|)+1.5\,\text{MeV}}, \\ Y_1^a(i) = -\dfrac{\frac{1}{2}\Omega_i^{1/2}\Lambda(+2)}{2(|\epsilon_i|-|\epsilon_{p_{1/2}}|)+5.32\,\text{MeV}}. \end{cases}$$

7

The corresponding numerical values are displayed in Tables 1.E.4 and 1.E.5 (see also Fig. 1.E.~~6~~).

B - B ← from p. 17

hematically

Appendix 1.F Microscopic mechanism to break gauge invariance

Pairing is intimately connected with particle number violation and thus spontaneous breaking of gauge invariance, as testified by the order parameter $\langle BCS|P^\dagger|BCS\rangle = \alpha_0$. Now, in the nuclear case and at variance with condensed matter, dynamical

Within the framework of Fig. 1.D.1 (parallel between 3D and gauge phenomena of spontaneous symmetry breaking), we display in Fig. 1.E.8, the relative importance of dynamic and static pairing distortions, in comparison with the corresponding quantities in the case of quadrupole surface distortions in ~~3~~ 3-D space.

These results underscore the major role pairing vibrations play in nuclei around closed shells.

49

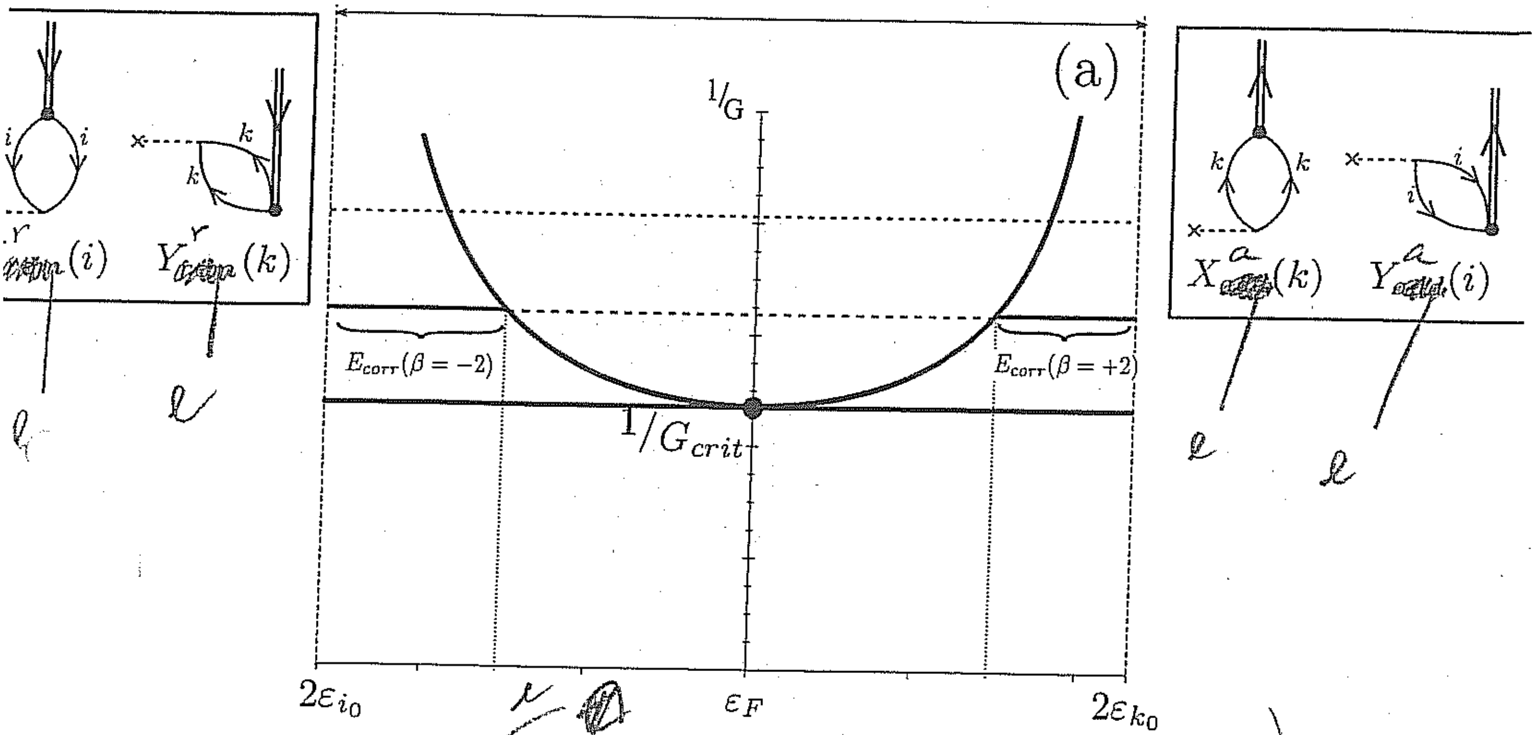

$\Delta = \sqrt{\Delta^2_{BCS} + \frac{1}{2} G^2 S_0(RPA)}$

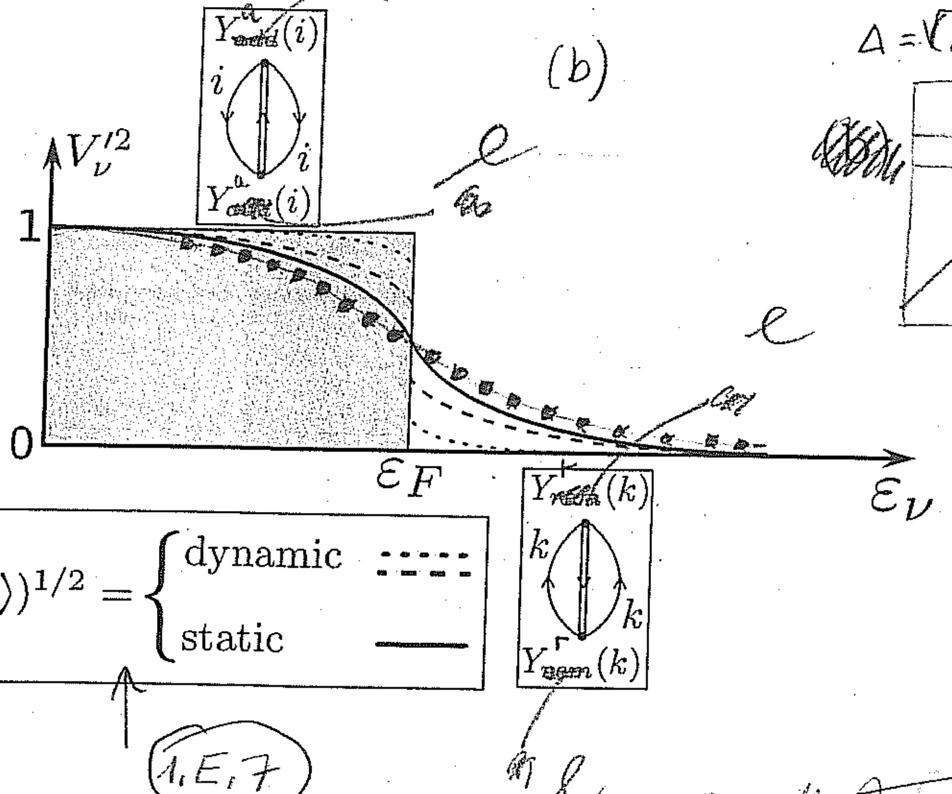

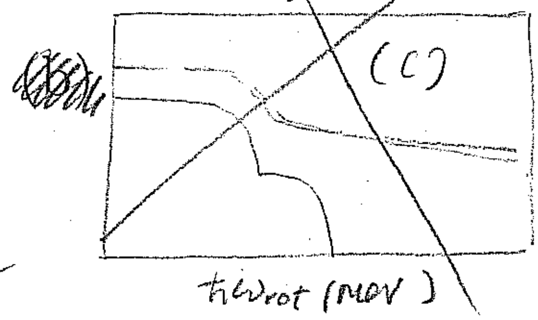

1, E, 8

$$(\langle 0|P^\dagger P|0\rangle)^{1/2} = \begin{cases} \text{dynamic} \\ \text{static} \end{cases}$$

1, E, 7

Fig. ~~1.1~~

1, E, 8

~~Fig. 1.2~~

$x = \frac{2G\Omega}{D} = G N(0)$

Fig. 2

150

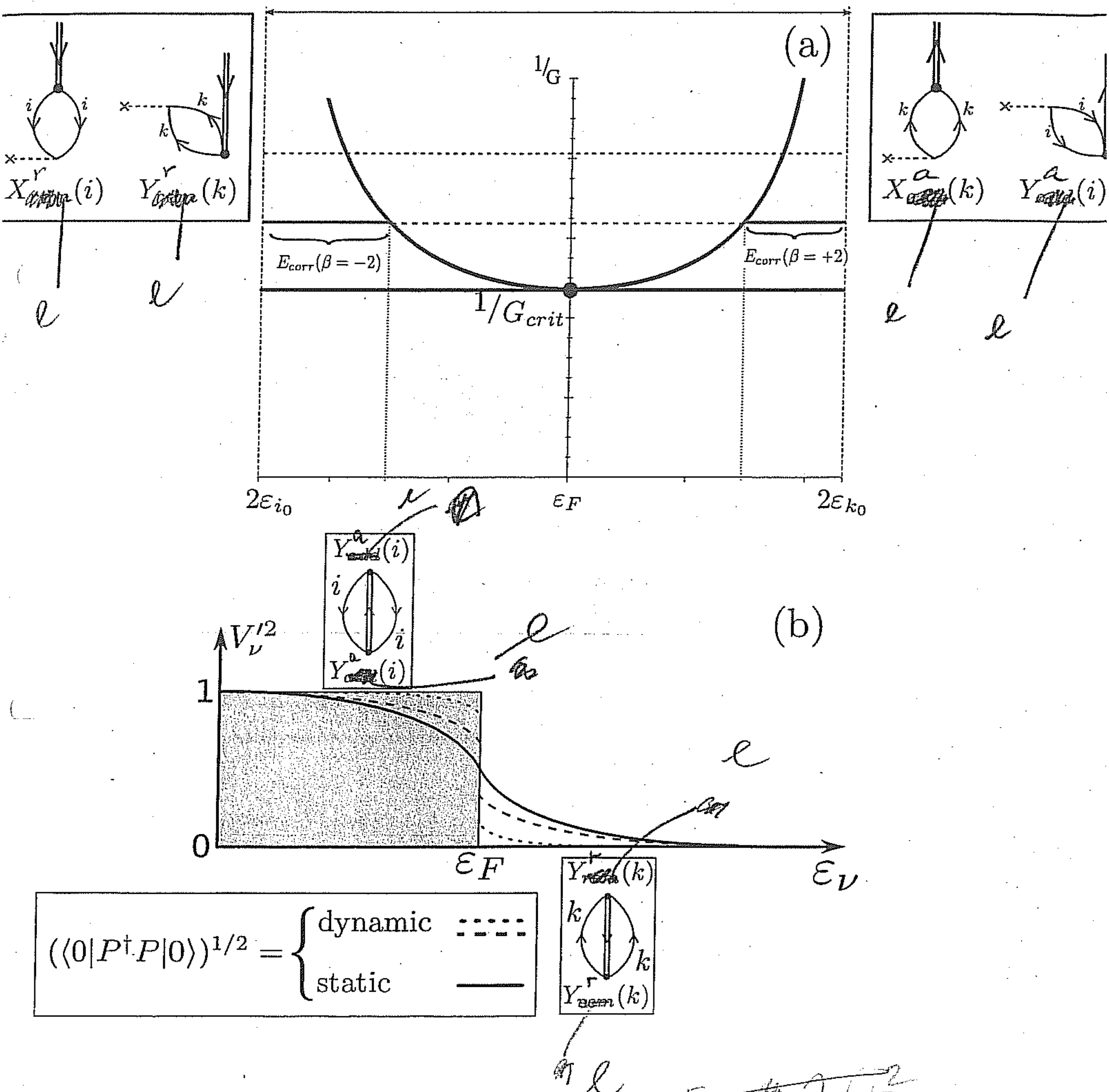

~~Fig. 2~~

FIG. 2

(57)

$$P^\dagger = \sum_{\nu>0} a^\dagger_\nu a^\dagger_{\bar\nu}$$

$$x = \frac{2G\Omega}{D} = GN(0)$$

$x > 1$	$x < 1$
$\alpha_0 = < P^\dagger > = \frac{\Delta}{G} \approx 7$	$\alpha_{dyn} = \frac{1}{G}\frac{<PP^\dagger>^{1/2}+<P^\dagger P>^{1/2}}{2}$ $\approx \frac{1}{2}\left(\frac{E_{corr}(A+2)}{G} + \frac{E_{corr}(A-2)}{G}\right) \approx 10$

$$\frac{\alpha_0}{\alpha_{dyn}} \approx 0.7$$

$$\frac{\beta_2}{(\beta_2)_{dyn}} \approx 3-6$$

1.E.8

Fig. 1.E.8

Relative importance of dynamic pairing distortion around closed shell and for pairing deformed nuclei, as compared with similar quantities for the case of quadrupole surface degrees of freedom.

(52)

units		MeV	MeV^{-1}	
nlj	Ω_k	$\lvert\epsilon_{g_{9/2}}\rvert - \lvert\epsilon_k\rvert$	$C(k) \overset{a)}{=} \frac{\frac{1}{2}\Omega_k^{1/2}}{2(\lvert\epsilon_{g_{9/2}}\rvert - \lvert\epsilon_k\rvert)+1.5\,\text{MeV}}$	$X_1^a(k)$
$1g_{9/2}$	5	0	0.745	0.82
$0i_{11/2}$	6	0.77	0.403	0.44
$0j_{15/2}$	8	1.41	0.327	0.36
$2d_{5/2}$	3	1.56	0.187	0.21
$3s_{1/2}$	1	2.03	0.090	0.10
$1g_{7/2}$	4	2.47	0.155	0.17
$2d_{3/2}$	2	2.51	0.108	0.12

√ Table 1.E.4: Forwards going RPA amplitudes associated with the pair addition mode of ^{208}Pb(cf Table XVI Broglia et al (1973))

a) $\sum_k C^2(k) = 0.903$

units		MeV	MeV^{-1}	
nlj	Ω_i	$\lvert\epsilon_i\rvert - \lvert\epsilon_{p_{1/2}}\rvert$	$D(i) \overset{a}{=} \frac{\frac{1}{2}\Omega_i^{1/2}}{2(\lvert\epsilon_i\rvert - \lvert\epsilon_{p_{1/2}}\rvert)+5.32\,\text{MeV}}$	$Y_1^a(i)$
$2p_{1/2}$	1	0	-0.094	-0.1
$1f_{5/2}$	3	0.57	-0.134	-0.15
$2p_{3/2}$	2	0.90	-0.099	-0.11
$0i_{13/2}$	7	1.64	-0.154	-0.17
$1f_{7/2}$	4	2.35	-0.100	-0.11
$0h_{9/2}$	5	3.47	-0.091	-0.10

√ Table 1.E.5: Same as Table 1.E.4 but for the backwards going amplitude.

a) $\sum_i D^2(i) = 0.079$; Thus $\Lambda^2(+2)(\sum_k C^2(k) - D^2(i)) = \Lambda^2(+2)(0.903 - 0.079)\,\text{MeV}^{-2}$
$= 0.824\,\text{MeV}^{-2}$; $\Lambda(+2) = \text{MeV}\,(0.824)^{-1/2} = 1.102\,\text{MeV}$;
$\Lambda(+2) = 1.102\,\text{MeV}$.

53

breaking of gauge symmetry is equally important (pairing vibrations around closed shell nuclei, cf. Fig. ??). The fact that the average single–particle field acts as an external potential (like e.g. magnetic field in metallic superconductors) is at the basis of the existence of a critical value of the pairing strength G to bind Cooper pairs in nuclei. In fact, spatial quantization in finite systems at large and in nuclei in particular, intimately connect with the tantamount role the surface has in these systems, is at the basis of the existence of a critical G value. Also of the fact that in nuclei an important fraction (30-50%) of Cooper pair binding is due to the exchange of collective vibrations between the partners of the pair, the rest being associated with the bare NN interaction in the ${}^1S_0$ channel (cf. Fig. ??).

Now, there are situations in which spatial quantization seems, essentially completely, the NN–interaction. This happens in the case in which the nuclear valence orbitals s, p–states at threshold (pairing anti halo effect). Examples of situations of this type are provided by $N = 6$ (parity inversion) isotones. In particular, by ^{11}Li, in which case the strongly renormalized $s1/2$ and $p1/2$ valence orbitals are a virual and a resonant stae lying at ≈0.1 and 0.6 MeV in the continuum, respectively. In keeping with the fact that the binding provided to a pair of fermions moving in time reversal states by a contact pairing interaction (δ–force) is (cf. e.g. Eq. (2.12) Brink and Broglia (2005)) $E_0 = (2j+1)/2V_0 I(j) \approx \frac{(2j+1)}{2} V_0 \frac{3}{R^3}$, the ratio

$$r = \frac{2}{(2j+1)} \left(\frac{R_0}{R}\right)^3,$$

where $R_0 = 1.2A^{1/3}$fm= 2.7fm ($A = 11$), and $R = \sqrt{\frac{5}{3}} \langle r^2 \rangle^{1/2}_{^{11}\mathrm{Li}} = \sqrt{\frac{5}{3}} 3.74$ fm =4.6 fm are the radius of a stable nucleus of mass $A = 11$ (systematics), while R is the measured one, while j is the angular momentum representative for a nucleus of mass $A = 11 (j \sim k_F R_0 \approx 3-4)$, one obtains $r = 0.06$. Making use of the multipole expansion of a general interaction

$$v(|\mathbf{r}_1 - \mathbf{r}_2|) = \sum_\lambda V_\lambda(r_1, r_2) P_\lambda(\cos\theta_{12}).$$

Because the function P_λ drops from its maximum at $\theta_{12} = 0$ in an angular distance $1/\lambda$, particles 1 and 2 interact through the component λ of the force, only if $r_{12} = |\mathbf{r}_1 - \mathbf{r}_2| < R/\lambda$, where R is the mean value of the radii $\mathbf{r}_1$ and $\mathbf{r}_2$. Thus, as λ increases, the effective force range decreases. For a force of range much greater than the nuclear size, only the $\lambda = 0$ term is important. At the other extreme, a δ–function force has coefficients $V_\lambda(r_1, r_2) \left(= \frac{(2\lambda+1)}{4\pi r_1^2} \delta(r_1 - r_2)\right)$ that increase with λ. In the case of ^{11}Li(gs) we are thus forced to accept the need for a long range, low λ pairing interaction, as responsible for the binding of the dineutron, halo Cooper pair to the ^{9}Li core. This is equivalent to saying, an induced pairing interaction arising from the exchange of vibrations with low λ–value.

1.F.1 Bootstrap Cooper pair binding

Within the s, p subspace, the most natural low wavelength vibration is the dipole mode. From systematics, the centroid of these vibrations is $\hbar\omega_{GDR} \approx 100\,\mathrm{MeV}/R$, R being the nuclear radius. Thus, in the case of ^{11}Li, one expects the centroid of the Giant Dipole Resonance carrying $\approx$100% of the energy weighted sum rule (EWSR) at $\hbar\omega_{GDR} \approx 100\,\mathrm{MeV}/2.7 \approx 37\,\mathrm{MeV}$. Now, such a high frequency mode can hardly be expected to give rise to anything, but polarization effects. On the other hand, there exists experimental evidence which testifies to the presence of a rather sharp dipole state with centroid at $\approx$ 1MeV and carrying $\approx$ 10% of the EWSR. The existence of this "pigmy resonance" which can be viewed as a simple consequence of the existence of a low–lying particle hole state associated with the transition $s_{1/2} \to p_{1/2}$, arguably, testifies to the coexistence of two states with rather different radii in the ground state[1]. One, closely connected with the ^{9}Li core, ($\approx$ 2.7fm), the second with the diffuse halo ($\approx$ 4.6 fm). Because the overlap between them s small ($\approx (2.7/4.6)^3 \approx 0.2$), one can posit that a bona fide dipole pigmy resonance is a GDR based on an exotic, unusually extended state as compared to systematics ($A \approx (4.6/1.2)^3 \approx 60$), i.e. to system with an effective A mass number about 5 times than predicted by systematics.

Let us try to shed some light on these issues. Making use of the relation $\langle r^2\rangle^{1/2} \approx (3/5)^{1/2}R$ between mean square radius and radius, one may write

$$\langle r^2\rangle_{^{11}\mathrm{Li}} \approx \frac{3}{5}R^2_{eff}(^{11}\mathrm{Li}).$$

with

$$R^2_{eff}(^{11}\mathrm{Li}) = \left(\frac{9}{11}R_0^2(^9\mathrm{Li}) + \frac{2}{11}\left(\frac{\xi}{2}\right)\right),$$

where

$$R_0^2(^9\mathrm{Li}) = 2.5\mathrm{fm}$$

is the ^{9}Li radius ($R_0 = r_0A^{1/3}, r_0 = 1.2$fm), where ξ is the correlation length of the Cooper pair neutron halo. An estimate of this quantity is provided by the relation

$$\xi = \frac{\hbar v_F}{2E_{corr}} \approx 20\mathrm{fm},$$

in keeping with the fact that in ^{11}Li, $(v_F/c) \approx 0.1$ and $E_{corr} \approx 0.5$MeV. Consequently, $\langle r^2\rangle^{1/2}_{^{11}\mathrm{Li}} \approx 3.74$fm ($R^{11}_{eff}Li\approx$ 4.83 fm), in overall agreement with the experimental value $\langle r^2\rangle^{1/2}_{^{11}\mathrm{Li}} = 3.55 \pm 0.1$fm (Kobayashi et al., 1989).

We now proceed to the calculation of the centroid of the dipole pigmy resonance of ^{11}Li. Making use of the dispersion relation given in Eq. (3.30) p.55 of **?**, and of the fact that $\epsilon_{\nu_k} - \epsilon_{\nu_i} = \epsilon_{p_{1/2}} - \epsilon_{s_{1/2}} \approx 0.5$MeV (see Fig. 11.1 p.264 Brink

[1] Within this context the dipole strength found at $\approx$ 10MeV in neutron skin rich nuclei can hardly be considered pigmy resonance, but the long tail of the GDR.

55

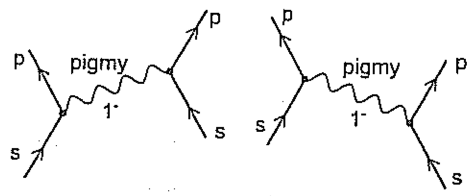

Figure 1.F.1:

and Broglia (2005)), and that the EWSR associated with the ^{11}Li pigmy resonance is $\approx$ 10% of the total Thomas–Reiche–Kuhn sum rule one can write,

$$0.1\frac{\hbar^2 A}{2M} = \frac{1}{\kappa_1}[(0.5\mathrm{MeV})^2 - (\hbar\omega_{pigmy})^2],$$

and thus

$$(\hbar\omega_{pigmy-})^2 = (0.5\mathrm{MeV})^2 0.1\frac{\hbar^2 A}{2M},$$

where (see ?)

$$\kappa_1 = \frac{5V_1}{A(\xi/2)^2}\left(\frac{2}{11}\right) = -\frac{125\mathrm{MeV}}{A100\mathrm{fm}^2}\left(\frac{2}{11}\right) \approx -\frac{2.5}{A^2}\mathrm{fm}^{-2}\mathrm{MeV},$$

the ratio in parenthesis reflecting the fact that only 2 out of 11 nucleons, slosh back and forth in an extended configuration with little overlap with the other nucleons. One then obtains,

$$-0.1\frac{\hbar^2 A}{2M}\kappa_1 = 0.1 \times 20\mathrm{MeV\ fm}^2 A \times \frac{2.5}{A^2}\mathrm{fm}^{-2}\mathrm{MeV} \approx 0.45\mathrm{MeV} \approx (0.7\mathrm{MeV})^2$$

consequently

$$\hbar\omega_{pigmy} = \sqrt{(0.5)^2 + (0.7)^2}\mathrm{MeV} \approx 1\mathrm{MeV},$$

in overall agreement with the experimental findings (?). It is of notice that the centroid of the pigmy resonance calculated in the RPA with the help of a separable interaction is $\approx$ (0.8MeV + 2.0MeV)/2 $\approx$ 1.4MeV (see Fig. 11.3(a) p.269, Brink and Broglia (2005). Let us now estimate the binding which the exchange of the pigmy resonance between two neutron of the Cooper pair halo of ^{11}Li can provide The associated particle vibration coupling $\Lambda\left(\partial W(E)/\partial E|_{\hbar\omega_{pigmy}}\right)^{-1/2}$, where $W(E)$ is the dispersion relation used to determine $\hbar\omega_{pigmy}$ (cf. e.g. Brink and Broglia (2005) Eq. (8.42) p.189; note the use of a dimensionless dipole single particle field $F' = F/\langle r^2\rangle_{^{11}\mathrm{Li}}$)

$$W(E) = \frac{2(\epsilon_k - \epsilon_i)|\langle\tilde{i}|F/\langle r^2\rangle_{^{11}\mathrm{Li}}|k\rangle|^2}{(\epsilon_k - \epsilon_i)^2 - E^2}$$

(56)

One then obtains

$$\Lambda^2 = \left\{ 2\hbar\omega_{pigmy} \frac{0.1(TRK)/\langle r^2\rangle_{^{11}\mathrm{Li}}}{\left[(\epsilon_{p_{1/2}-\epsilon_{s_{1/2}}})^2 - (\hbar\omega_{pigmy})^2\right]^2} \right\}^{-1}$$
$$= \left\{ 2\mathrm{Mev} \frac{0.1(\hbar^2 A/2M)(1/\langle r^2\rangle_{^{11}\mathrm{Li})}}{[(0.5)^2 - (1\mathrm{MeV})^2]^2\,\mathrm{MeV}^4} \right\}^{-1}$$
$$= \left(\frac{0.75}{1.57}\right)^2 = 0.48\mathrm{MeV}^2$$

leading to $\Lambda = 0.7$MeV. The value of induced interaction matrix elements is then given by

$$M_{ind} = -\frac{\Lambda^2}{\hbar\omega_{pigmy}} = -0.5\mathrm{MeV},$$

and the same contribution for the other time ordering. Assuming the halo neutrons to spend the same amount of time in the $|s^2_{1/2}(0)\rangle(\epsilon_{s_{1/2}} = 0.1$ MeV) than in the $|p^2_{1/2}(0)\rangle(\epsilon_{p_{1/2}} = 0.6$ MeV) configuration, the correlation energy is $E_{corr} = |2(\epsilon_{s_{1/2}} + \epsilon_{p_{1/2}})/2 + 2M_{ind}| = 0.3$ MeV, in overall agreement with the findings (0.380 MeV).

New version June 11th, 2014

57

Bibliography

D. R. Bès and R. A. Broglia. Pairing vibrations. *Nucl. Phys.*, 80:289, 1966.

P. Bortignon, A. Bracco, and R. Broglia. *Giant Resonances.* Harwood Academic Publishers, Amsterdam, 1998.

D. Brink and R. A. Broglia. *Nuclear Superfluidity.* Cambridge University Press, Cambridge, 2005.

R. Broglia, O. Hansen, and C. Riedel. Two–neutron transfer reactions and the pairing model. *Advances in Nuclear Physics*, 6:287, 1973. URL `http://merlino.mi.infn.it/repository/BrogliaHansenRiedel.pdf`.

C. Mahaux et al. Dynamics of the shell model. *Physics Reports*, 120:1–274, 1985.

T. Kobayashi, S. Shimoura, I. Tanihata, K. Katori, K. Matsuta, T. Minamisono, K. Sugimoto, W. Mller, D. L. Olson, T. J. M. Symons, and H. Wieman. Electromagnetic dissociation and soft giant dipole resonance of the neutron-dripline nucleus ^{11}Li. *Physics Letters B*, 232:51, 1989.

G. Potel, A. Idini, F. Barranco, E. Vigezzi, and R. A. Broglia. Cooper pair transfer in nuclei. *Rep. Prog. Phys.*, 76:106301, 2013.

M. Zinser, F. Humbert, T. Nilsson, W. Schwab, H. Simon, T. Aumann, M. J. G. Borge, L. V. Chulkov, J. Cub, T. W. Elze, H. Emling, H. Geissel, D. Guillemaud-Mueller, P. G. Hansen, R. Holzmann, H. Irnich, B. Jonson, J. V. Kratz, R. Kulessa, Y. Leifels, H. Lenske, A. Magel, A. C. Mueller, G. Mnzenberg, F. Nickel, G. Nyman, A. Richter, K. Riisager, C. Scheidenberger, G. Schrieder, K. Stelzer, J. Stroth, A. Surowiec, O. Tengblad, E. Wajda, and E. Zude. Invariant-mass spectroscopy of ^{10}Li and ^{11}Li. *Nuclear Physics A*, 619:151, 1997.

58

Bibliography

D. Brink and R. A. Broglia. *Nuclear Superfluidity*. Cambridge University Press, Cambridge, 2005.

R. Broglia, O. Hansen, and C. Riedel. Two–neutron transfer reactions and the pairing model. *Advances in Nuclear Physics*, 6:287, 1973. URL `http://merlino.mi.infn.it/repository/BrogliaHansenRiedel.pdf`.

T. Kobayashi, S. Shimoura, I. Tanihata, K. Katori, K. Matsuta, T. Minamisono, K. Sugimoto, W. Mller, D. L. Olson, T. J. M. Symons, and H. Wieman. Electromagnetic dissociation and soft giant dipole resonance of the neutron-dripline nucleus ^{11}Li. *Physics Letters B*, 232:51, 1989.

G. Potel, A. Idini, F. Barranco, E. Vigezzi, and R. A. Broglia. Cooper pair transfer in nuclei. *Rep. Prog. Phys.*, 76:106301, 2013.